THE EUROPEAN
PHYSICAL JOURNAL C

Coherent elastic nuclear scattering of ^{51}Cr neutrinos

C. Bellenghi[1,2], **D. Chiesa**[3,4], **L. Di Noto**[5,6], **M. Pallavicini**[5,6], **E. Previtali**[3,4], **M. Vignati**[2,a]

[1] Dipartimento di Fisica, Sapienza Università di Roma, Rome 00185, Italy
[2] INFN Sezione di Roma, Rome, Italy
[3] Dipartimento di Fisica, Università di Milano - Bicocca, Milano 20126, Italy
[4] INFN Sezione di Milano Bicocca, Milano, Italy
[5] Dipartimento di Fisica, Università di Genova, Genova 16146, Italy
[6] INFN Sezione di Genova, Genova, Italy

Abstract Searches for new physics in the coherent elastic neutrino-nucleus scattering require a precise knowledge of the neutrino flux and energy spectrum. In this paper we investigate the feasibility and the performance of an experiment based on a ^{51}Cr source, whose neutrino spectrum is known and whose activity can be heat-monitored at few permil level. With a 5 MCi source placed at $\sim$ 25 cm from the detector, under an exposure of two ^{51}Cr half-lives (55.4 days), we evaluate 3900 (900) counts on a 2000 cm^3 target of germanium (sapphire) featuring an energy threshold of 8 (20) eV. To further increase the exposure, multiple activations of the same source could be possible.

1 Introduction

Predicted in 1973 [1] and observed for the first time in 2017 [2], the coherent elastic neutrino-nucleus scattering (CEνNS) has been proposed to search for neutrino magnetic moment, Z' exchange, non-standard interactions, sterile neutrinos [3–7], and to perform precision measurements of the nuclear form factor [8] and of $\sin^2 \theta_W$ at low momentum transfer [9]. The advantage of CEνNS relies in the relatively large neutrino cross section, which scales quadratically with the number of neutrons in the nucleus [10]:

$$\frac{d\sigma}{dT} = \frac{G_F^2}{4\pi} F^2(q^2) Q_W^2 M_A \left(1 - \frac{M_A T}{2E_\nu^2} \right) \qquad (1)$$
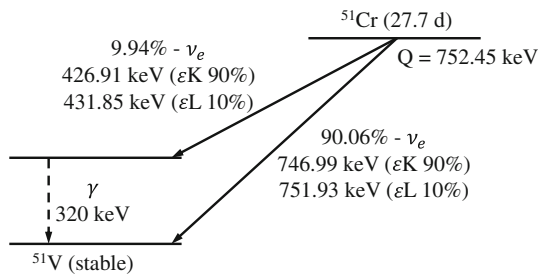
where G_F is the Fermi constant, F the nuclear form factor, $Q_W = N - Z(1 - 4\sin^2 \theta_W) \simeq N$, N the number of neutrons in the nucleus, Z the number of protons, θ_W the Weinberg angle, M_A the nucleus mass, T the nucleus recoil

[a] e-mail: marco.vignati@roma1.infn.it

energy and E_ν the neutrino energy. On the other hand, the recoil energy $T \leq 2E_\nu^2/M_A$ is small, of the order of tens or hundreds of eV for MeV neutrinos on a Germanium target. To achieve small energy thresholds, germanium diodes [11–13], CCD's [14,15], and cryogenic phonon detectors of silicon, germanium [16,17], sapphire and CaWO$_4$ [18] have been proposed. The most competitive thresholds have been demonstrated by phonon detectors (tens of eV) and CCDs (1 electron).

Current searches for new physics in CEνNS could be limited by systematic errors on the neutrino flux and energy spectrum, as in the case of neutrino spallation sources, where the flux normalization precision is currently $\sim$ 10% [2], and power nuclear reactors, where models of the neutrinos emitted by the nuclear fuel limit the precision to several percent [19,20]. Instead, artificial nuclear sources can be characterized with high precision and were already employed in the past in the GALLEX (^{51}Cr) [21] and SAGE (^{51}Cr, ^{37}Ar) [22] experiments, and recently proposed by the SOX experiment (^{144}Ce) [23] which, however, was stopped by difficulties occurred during the isotope mass production.

In this paper we set the requirements for an experiment on CEνNS with a high-intensity source of ^{51}Cr, an electron-capture decaying isotope with a half-life of 27.7 days. The neutrino spectrum consists of four monochromatic lines, including the most energetic 747 keV (81%) and 752 keV (9%) lines which can be exploited for the coherent elastic neutrino-nucleus observation (see the complete decay scheme in Fig. 1). One advantage of this choice consists in the possibility of reusing the source of the GALLEX experiment, which is still owned by INFN: 36 kg of Cromium 38.6% enriched in ^{50}Cr, that need to be activated at a nuclear reactor. Another advantage consists in the possibility of measuring the activity at few per mill level with small modifications of the thermal calorimeter already developed by SOX

Fig. 1 ^{51}Cr decay scheme [25]

Fig. 2 Differential cross section as a function of recoil energy T for ^{51}Cr neutrinos on typical targets used in cryogenic experiments: silicon, germanium, sapphire and calcium tungstate. The nuclear form factor in Eq. 1 is assumed unitary [29]

for its ^{144}Ce source [24]. Additionally, the detection of neutrinos produced by the electron capture could provide complementary information to the detection of anti-neutrinos from nuclear reactors.

After reviewing the possibilities to activate the source, studying its gamma-ray shield and the activity measurement, we propose an experimental configuration placing the source as close as ~ 25 cm to the detector. Given that the maximum recoil energy amounts to tens of eV (Fig. 2), only the case of cryogenic phonon detectors is considered. CCDs are also highly promising, provided that the energy conversion efficiency of nuclear recoils to electrons is precisely measured.

2 Activation of the Cr sample

We take as reference the irradiation performed in 1994 to produce the 1.7 MCi source of GALLEX [21,26]. This source was obtained by neutron activation of the full sample of 36 kg of Cr, in the form of ~ 1 mm^3 metal chips, with a total number of ^{50}Cr nuclei amounting to 1.6×10^{26}. The irradiation was performed at the Siloé reactor in Grenoble, nowadays decommissioned, and lasted 23.8 days. The reactor core was specially reconfigured to host zircalloy containers for the Cr chips, that were exposed to an average thermal neutron flux of 5.2×10^{13} n/cm^{2}s. This number was directly measured during the activation and takes into account the perturbation of the neutron flux due to the self-shielding of the Cr sample. The value of the unperturbed neutron flux is not available in literature however we can refer to the IAEA's Research Reactor Database [27], where the maximum total flux of the Siloé reactor is quoted in the range $2 - 4 \times 10^{14}$ n/cm^{2}s.

In the following we survey some of the possible sites to activate the source. Power reactors are not suitable, because they have no internal sites to place irradiation targets. Conversely, some research reactors have facilities which in principle are suitable in terms of neutron flux and space available to fit the Cr target. We restrict the list to sites with high neutron fluxes, in order to activate the largest possible number of nuclei.
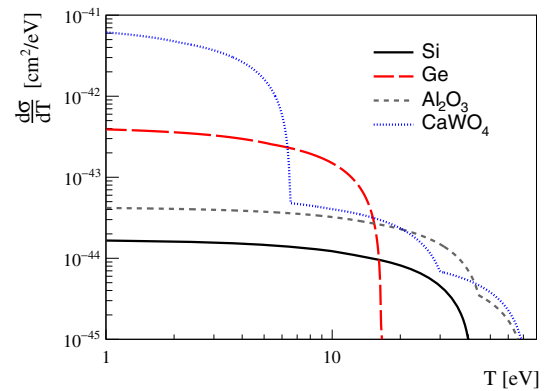
– The BR2 reactor at Mol (Belgium), is not only one of the most powerful (up to 100 MW) material testing reactor in the world, but also a major facility for radioisotope production. The reactor, whose core is 80 cm high, has a 20 cm $\varnothing$ *central large channel*, with maximum thermal neutron flux 10^{15} n/cm^{2}s, and 3 *peripheral large channels* with 3×10^{14} n/cm^{2}s. The typical cycle is three weeks [28].

– The High Flux Isotope Reactor (HFIR) at Oak Ridge (USA), 85 MW power, has irradiation positions with thermal fluxes up to 1.2–2.5×10^{15} n/cm^{2}s, however irradiations must be carefully reviewed with respect to their neutron poison content, which is limited because of their adverse effects on the reactor power distribution and fuel cycle length [30]. Nevertheless HFIR has also 16 small (4 cm $\varnothing$) and 6 large (7.2 cm $\varnothing$) *vertical experiment facilities* (VXF), 50 cm high, with maximum thermal neutron flux in the range 4–7×10^{14} n/cm^{2}s. Large neutron poison loads in VXF facilities are of no particular concern [31].

– Other reactors with similar features are the Advanced Test Reactor (ATR) at Idaho National Laboratory (USA), the HFR reactor at Petten (Netherlands), and the SM3 or MIR.M1 reactors at Dimitrovgrad (Russia). The Jules Horowitz Reactor (JHR), currently under construction in Cadarache (France) will feature facilities in the reflector region with thermal fluxes up to 5×10^{14} n/cm^{2}s [32].

Considering an average unperturbed thermal neutron flux of 5×10^{14} n/cm^{2}s, we calculated the activity that would be obtained after 24 days of irradiation of the Cr target. We performed Monte Carlo simulations with the MCNP code [33] to evaluate the self-shielding effect in different irradiation geometries and obtained an activity in the range of 3.5–7 MCi.

In the following we assume the activity of ^{51}Cr as 5 MCi. If not sufficient, the source could be re-activated several times, since the number of ^{50}Cr isotopes transmuted would correspond to the 0.4% only of the GALLEX sample. Increasing the irradiation time instead is not obvious, because irradiation cycles of research reactors typically last three weeks.

3 Source shielding and activity measurement

^{51}Cr produces only 320 keV gammas in 10% of the decays that, from the safety point of view, can be easily shielded by a few centimeters of tungsten. The most worrisome radiation, instead, comes from the sample impurities. In GALLEX, despite the special care taken in all the chemical processing stages, impurities with (n,γ) cross section in the barn range were activated during irradiation, producing radionuclides with lifetime of several days. In particular, the 1.3–1.5 MeV γ emitter ^{110m}Ag ($T_{1/2}$ = 150 days) was found with an activity of 4 GBq [34], while other long-lived emitters such as ^{46}Sc (1.2 MeV), ^{60}Co (1.1–1.3 MeV) and ^{124}Sb (2 MeV) were found with an activity smaller than 0.5 GBq [26]. Assuming the same activation factor of GALLEX, an activity around 12 GBq is expected from a 5 MCi source. To comply the safety rules (dose at contact < 100–200 uSv/h), an attenuation factor > 2000 is necessary, which could be achieved with a shield of tungsten at least 8 cm thick.

The γs escaping the shield may reach the detector and generate a continuum background down to the signal region via Compton scattering. Aside the impurities, the ^{51}Cr would produce γs up to $\sim$ 750 keV via inner bremsstrahlung which, even if suppressed by a factor 7×10^{-4}, is still abundant in a 5 MCi source (185 PBq). The purification level of the source and the shield thickness needed to not overwhelm the neutrino signal depend on the geometry of the experiment and on the detector materials, and are analysed in the next section.

Since the 320 keV γ, the X and Auger radiations are completely absorbed and the heat released by impurities is negligible, a total of (36.51± 0.161) keV is liberated per each ^{51}Cr decay, corresponding to 422 W for a 5 MCi source. To measure the activity, just before and after the data taking, the shielded source can be inserted inside a thermal heat exchanger in which ultra-pure water circulates and eventually absorbs the heat, increasing its temperature. As it has been shown in Ref. [24] for the case of ^{144}Ce, the thermal losses due to the convection, conduction and irradiation can be minimized at negligible levels. By measuring the mass flow and the inlet and outlet water temperatures, the heat power can be evaluated with 0.2% precision. Since the ^{51}Cr half-life is about 10 times shorter than the ^{144}Ce half-life for which the apparatus was designed and calibrated, a systematic shift of about 0.5% in the measured power arises, due to the delay

time induced by the heat propagation from the source to the water. Nevertheless the delay time can be decreased by improving the thermal contact between the shielded source and the heat exchanger, or it can be measured during the calibration phase, allowing the precision to be preserved at few per mill level.

4 Prototype experiment

Next generation phonon detectors for dark matter and CEνNS search aim at kg detectors with energy threshold of tens of eV. An energy threshold of 20 eV has been already demonstrated on a 0.5 g (5 × 5 × 5 mm^3) sapphire target [35], while 60 eV have been demonstrated on a 33.4 g (20 mm $\varnothing$ × 20 mm) germanium target [36]. The challenge consists in scaling up the technology to thousands detectors, by improving the detector reproducibility and the multiplexing capability. While it is customary to quantify the size of the detector by its mass, here we choose to fix its volume, since in cryogenic experiments the technology scale up depends mainly on the size and number of detectors, irrespective of their density, and since in the setup we are proposing the neutrino flux depends on the detector geometry. We choose a volume of 2000 cm^3, which corresponds to $\sim$ 5 − 12 kg depending on the target considered, and we choose a cylindrical shape with 10 cm diameter.

To maximize the neutrino flux we place the source as close as possible to the detector. Custom cryostat tails can be realized with a thickness of $\sim$ 5 cm between the low temperature volume hosting the detector and the outside. The source, surrounded by its shield, is then placed around the cryostat, in a toroidal configuration. We perform simulations to determine the source height and thickness that maximize the neutrino flux, keeping the volume fixed to the GALLEX measured value of 10000 cm^3. To determine the shield thickness we also simulate the irreducible γ background from the inner bremsstrahlung of ^{51}Cr, restricting to Sapphire targets. Figure 3 sketches the proposed configuration of the experiment, where we also allow for 1 cm tolerance between the detector and the inner cryostat shield and between the outer cryostat shield and the source shield. The internal thickness of the tungsten shield that ensures a background one order of magnitude below the neutrino signal is 12 cm. The external thickness is fixed to the safety requirement of 8 cm. The source height and thickness that maximize the neutrino flux are 25 and 2.5 cm, respectively.

The neutrino flux at the detector, averaged over two ^{51}Cr half-lives, ranges between 1.0 and 1.2 × 10^{13} ν/cm^{2}s depending on the impact position, with an average of 1.1 × 10^{13} ν/cm^{2}s. The counts registered in the detector as a function of its energy threshold, for the targets used in present experiments, are shown in Fig. 4. With a threshold of 20 eV,
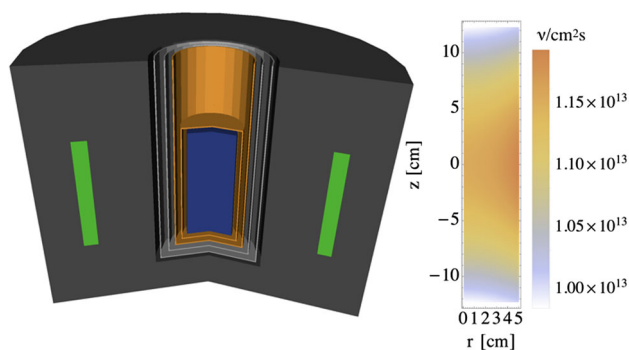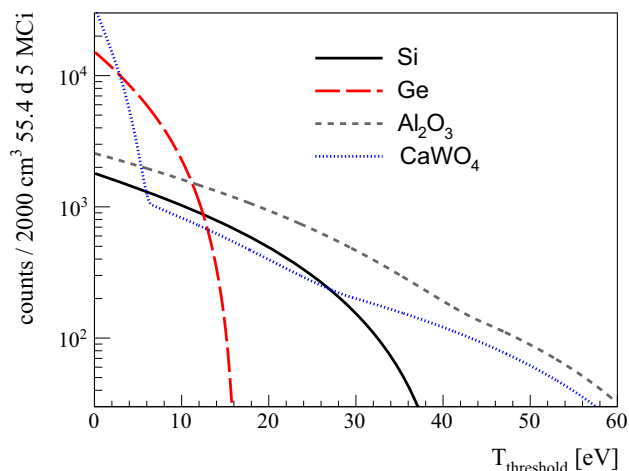
Fig. 3 Left: cylindrical detector of 2000 cm^3 with 5 cm radius (blue), placed inside a cylindrical cryostat 5 cm thick (orange - light gray). The 10000 cm^3 source (green) is deployed in a toroid around the cryostat and shielded in the radial direction by 12 cm of tungsten (dark gray). The source is at an average distance of 25 cm from the detector center, and its height (25 cm) is chosen to maximize the neutrino flux. Right: simulation of the neutrino flux at the detector in cylindrical coordinates for a ^{51}Cr source with initial activity of 5 MCi averaged over 2 half-lives (55.4 days)

Fig. 4 Counts above threshold for different types of 2000 cm^3 detectors from 55.4 days of exposure to a source of 5 MCi initial activity, in the same experimental configuration of Fig. 3

sapphire detectors would register 900 counts, corresponding to a 3.3% precision on the cross-section measurement without considering backgrounds. In case the detector technology advances and pushes down the threshold, a germanium target would register 3900 counts with a threshold of 8 eV, corresponding to a 1.6% precision. Silicon would provide a factor 2 lower counts than sapphire whereas calcium tungstate, to overcome the germanium performance, would require an energy threshold below 3 eV, a value that appears difficult to achieve.

The background at low energies due to Compton scattered γs must be studied with detailed measurements and simulations. With our Geant4-based simulation we estimated that, with a 12 cm tungsten shield, Ag impurities in the GALLEX sample must be reduced from ppm to ppb to not generate a background.[1] The environmental background is hard to predict since there are no measurements at such low energies: experiments will hopefully start soon, and provide key information. The most worrisome background could be due to neutrons, which could be absorbed with additional shielding.

To increase the exposure, aside the increase of the detector size, rerunning the same experiment is in principle possible. As described in Sect. 2, the Cr sample could be exposed back to neutrons and the experiment could restart. In this view, and also considering the short half-life, the experiment should be performed close to the nuclear reactor complex where the source is activated. For a 100 MW reactor, neutrinos from the core would appear as a continuum background 10 times

smaller than the signal if the experiment is located at a distance greater than 25 m.

Data Availability Statement This manuscript has no associated data or the data will not be deposited. [Author's comment: Paper not based on experimental data.]

---

[1] The Geant4 simulation we use is not trustworthy at energies below 1 keV. We extrapolate the continuum generated by Compton scattering in the region $1 - 10$ keV down to the neutrino signal region, which is below 60 eV. Dedicated measurements are needed to measure and simulate the physical processes taking place at such low energies.

References

1. D.Z. Freedman, Phys. Rev. D **9**, 1389 (1974). https://doi.org/10.1103/PhysRevD.9.1389
2. D. Akimov et al., Science **357**(6356), 1123 (2017). https://doi.org/10.1126/science.aao0990
3. A.C. Dodd, E. Papageorgiu, S. Ranfone, Phys. Lett. B **266**, 434 (1991). https://doi.org/10.1016/0370-2693(91)91064-3
4. J. Barranco, O.G. Miranda, T.I. Rashba, JHEP **12**, 021 (2005). https://doi.org/10.1088/1126-6708/2005/12/021
5. J.A. Formaggio, E. Figueroa-Feliciano, A.J. Anderson, Phys. Rev. D **85**, 013009 (2012). https://doi.org/10.1103/PhysRevD.85.013009
6. B. Dutta, Y. Gao, R. Mahapatra, N. Mirabolfathi, L.E. Strigari, J.W. Walker, Phys. Rev. D **94**(9), 093002 (2016). https://doi.org/10.1103/PhysRevD.94.093002

7. M. Lindner, W. Rodejohann, X.J. Xu, JHEP **03**, 097 (2017). https://doi.org/10.1007/JHEP03(2017)097

8. K. Patton, J. Engel, G.C. McLaughlin, N. Schunck, Phys. Rev. C **86**, 024612 (2012). https://doi.org/10.1103/PhysRevC.86.024612

9. J. Erler, R. Ferro-Hernández, JHEP **03**, 196 (2018). https://doi.org/10.1007/JHEP03(2018)196

10. D.Z. Freedman, D.N. Schramm, D.L. Tubbs, Ann. Rev. Nucl. Part. Sci. **27**, 167 (1977). https://doi.org/10.1146/annurev.ns.27.120177.001123

11. P.S. Barbeau, J.I. Collar, O. Tench, JCAP **0709**, 009 (2007). https://doi.org/10.1088/1475-7516/2007/09/009

12. J. Hakenmüller, et al., arXiv:1903.09269 (2019)

13. S. Kerman, V. Sharma, M. Deniz, H.T. Wong, J.W. Chen, H.B. Li, S.T. Lin, C.P. Liu, Q. Yue, Phys. Rev. D **93**(11), 113006 (2016). https://doi.org/10.1103/PhysRevD.93.113006

14. A. Aguilar-Arevalo et al., J. Phys. Conf. Ser. **761**(1), 012057 (2016). https://doi.org/10.1088/1742-6596/761/1/012057

15. J. Tiffenberg, M. Sofo-Haro, A. Drlica-Wagner, R. Essig, Y. Guardincerri, S. Holland, T. Volansky, T.T. Yu, Phys. Rev. Lett. **119**(13), 131802 (2017). https://doi.org/10.1103/PhysRevLett.119.131802

16. G. Agnolet et al., Nucl. Instrum. Methods **A853**, 53 (2017). https://doi.org/10.1016/j.nima.2017.02.024

17. J. Billard et al., J. Phys. G **44**(10), 105101 (2017). https://doi.org/10.1088/1361-6471/aa83d0

18. R. Strauss et al., Eur. Phys. J. C **77**, 506 (2017). https://doi.org/10.1140/epjc/s10052-017-5068-2

19. A.C. Hayes, J.L. Friar, G.T. Garvey, G. Jungman, G. Jonkmans, Phys. Rev. Lett. **112**, 202501 (2014). https://doi.org/10.1103/PhysRevLett.112.202501

20. A.C. Hayes, P. Vogel, Annu. Rev. Nuclear Part. Sci. **66**(1), 219 (2016). https://doi.org/10.1146/annurev-nucl-102115-044826

21. P. Anselmann et al., Phys. Lett. B **342**(1), 440 (1995). https://doi.org/10.1016/0370-2693(94)01586-2

22. J.N. Abdurashitov et al., Phys. Rev. C **59**, 2246 (1999). https://doi.org/10.1103/PhysRevC.59.2246

23. G. Bellini et al., JHEP **08**, 038 (2013). https://doi.org/10.1007/JHEP08(2013)038

24. K. Altenmüller et al., JINST **13**(09), P09008 (2018). https://doi.org/10.1088/1748-0221/13/09/P09008

25. M. Martin. Nucl. Data Sheets 144, 1 (2017). https://www.nndc.bnl.gov/ensdf/DatasetFetchServlet. Accessed: 2019-05-10

26. M. Cribier et al., NIM A **378**(1), 233 (1996). https://doi.org/10.1016/0168-9002(96)00464-0

27. IAEA's Research Reactor Database. https://nucleus.iaea.org/Pages/rr-db.aspx. Accessed: 2019-04-15

28. S.V. Dyck, G.V.D. Branden. The restart of the BR2 reactor after its third refurbishment. Proceedings of the European Research Reactor Conference – RRFM 2017. https://www.euronuclear.org/meetings/rrfm2017/pdf/fullpapers/RRFM2017-A0032.pdf. Accessed: 2019-04-15

29. D. Aristizabal Sierra, J. Liao, D. Marfatia, arXiv:1902.07398 (2019)

30. High Flux Isotope Reactor (HFIR), Oak Ridge National Laboratory, Department of Energy. https://neutrons.ornl.gov/sites/default/files/HighFluxIsotopeReactorUserGuide2.0.pdf. Accessed: 2019-04-15

31. R. Konings, T. Allen, R. Stoller, S. Yamanaka, *Comprehensive Nuclear Materials* (Elsevier Science, 2011)

32. Y. Bergamaschi, et al. Jules horowitz reactor, basic design. Proceedings of 2002 International Meeting on Reduced Enrichment for Research and Test Reactors. https://www.rertr.anl.gov/Web2002/2003Web/Bergamaschi.html. Accessed: 2019-04-15

33. X-5 Monte Carlo Team, *MCNP - A General Monte Carlo N-Particle Transport Code, Version 5*. Los Alamos National Laboratory (2008)

34. E. Bellotti, C. Cattadori, O. Cremonesi, N. Ferrari, E. Fiorini, S. Latorre, NIM B **100**(1), 199 (1995). https://doi.org/10.1016/0168-583X(95)00269-3

35. R. Strauss et al., Phys. Rev. D **96**(2), 022009 (2017). https://doi.org/10.1103/PhysRevD.96.022009

36. E. Armengaud et al., Phys. Rev. D **99**(8), 082003 (2019). https://doi.org/10.1103/PhysRevD.99.082003